

# An Electron Paramagnetic Resonance Study of Some Metal Ions in Guanidinium Aluminum Sulfate Hexahydrate

Robert W. Schwartz and Richard L. Carlin\*

Contribution from the Department of Chemistry,  
University of Illinois at Chicago Circle, Chicago, Illinois 60680.

Received April 24, 1970

**Abstract:** The electron paramagnetic resonance spectra of a number of trivalent iron-series ions in GASH down to liquid helium temperatures are reported. While the host crystal normally exhibits only two different magnetic sites, we find for titanium a large number of resonance lines and assign these to a variety of distorted lattice sites. These different sites arise as a result of local strain in the lattice caused by the large size of the titanium ions. Some sites are identified from the  $g$  values as having a negative trigonal field ( $v < 0$ ) and a  ${}^2A$  ground state. Others have  $v > 0$  and a  ${}^2E$  ground state, within which we propose that a transition occurs between components of two different Kramer's doublets. For vanadium the  $\Delta m_s = \pm 2$  transition is reported and we find that the electron spin cannot be approximated as quantized along the symmetry axis, despite the fact that  $D$  is much greater than  $g\beta H$ . These conditions lead to a unique intensity pattern in the hyperfine structure, and we find good agreement between theory and experiment. The nuclear hyperfine interaction of  $Cr^{3+}$  in GASH is about 16 G. Many extra lines are observed for  $Cr^{3+}$  and these are assigned as resulting from an exchange interaction between near-neighbor ions.

In an effort to understand better those factors which determine the electronic structure (*i.e.*, the electronic energy levels) of transition metal ions in crystals, a complete optical and magnetic study of a series of these ions in similar crystal symmetries has been undertaken. It was decided to investigate a series of hexaquo trivalent ions in crystals where a trigonal distortion is present. By studying the changes as different metals are substituted into the same lattice and one metal is substituted into related lattices a total picture might be obtained. This process involves replacing some, or all, of a nonmagnetic, colorless metal ion of a host crystal with the appropriate magnetic ion.

We have chosen the interesting ferroelectric, guanidinium aluminum sulfate hexahydrate, henceforth GASH,  $[C(NH_2)_3]Al(SO_4)_2 \cdot 6H_2O$ , as the nonmagnetic host, and have earlier<sup>1,2</sup> reported the polarized optical spectra of the trivalent iron-series ions in this crystal at 20°K. Several ambiguities arose in the interpretation of the spectra which were not resolved by our preliminary magnetic measurements on powders;<sup>3</sup> for example, the visible bands of trivalent titanium were not polarized strongly enough to determine either the sign or the magnitude of the trigonal field parameter  $v$ . The uncertainties can be resolved in some cases by a careful examination of the properties of the ground state of the magnetic ion, and this paper serves as our first report on the nature of the ground states and zero-field splittings of ions in GASH as evidenced by their magnetic properties at low temperatures.

## Experimental Section

Crystals of GASH and its gallium isomorph, GGaSH, have been grown by slow evaporation of the requisite aqueous solutions as reported earlier.<sup>1</sup> Epr spectra have been recorded at 4.2, 77, and 300°K on a Jeolco JES-3BS X-band spectrometer, which utilizes 100-kHz modulation at ambient and liquid nitrogen temperatures, and 80-Hz modulation at the temperature of boiling helium. DPPH and an internal frequency meter served as the field calibrants.

\* Address correspondence to this author.

(1) R. L. Carlin and I. M. Walker, *J. Chem. Phys.*, **46**, 3921 (1967).  
(2) I. M. Walker and R. L. Carlin, *ibid.*, **46**, 3931 (1967).  
(3) R. L. Carlin and E. G. Terezakis, *ibid.*, **47**, 4901 (1967).

The crystal structure of uniaxial GASH has been reviewed earlier,<sup>1</sup> and the recent redetermination<sup>4</sup> of the structure of GASH and its chromium isomorph has also been of use to us. The only points concerning the structure that require reemphasis are that, of the three molecules in the unit cell, only two are crystallographically and magnetically equivalent, and both octahedral sites have their threefold molecular axis along the crystal  $c$  axis.

## Results and Methods of Analysis

**1. Titanium.** No epr spectrum of  $Ti^{3+}$ :GASH has previously been reported, although an attempt to measure it has been made.<sup>5</sup> This spin- $1/2$  system is described by the spin Hamiltonian  $\mathcal{H} = \beta \mathbf{H} \cdot \mathbf{g} \cdot \mathbf{S}$ , which reduces to  $g\beta H S_z$ , where  $g^2 = g_{\parallel}^2 \cos^2 \theta + g_{\perp}^2 \sin^2 \theta$  and  $\theta$  is the angle between the molecular axis and the external field. One resonance line from each magnetic site is anticipated, and the resonance condition is simply

$$h\nu = g(\theta)\beta H \quad (1)$$

The spectrum can be observed only at 4.2°K. The lowest energy levels and epr spectra of  $Ti^{3+}$ :GASH are illustrated in Figures 1-5. The features may be summarized as follows. (a) In a concentrated (1-5%) sample, there are numerous lines, four or five being more intense than the others. Two different concentrated samples exhibited similar spectra at  $\theta = 0^\circ$ . All but one resonance in one sample had an almost random distribution of  $H_{res}$  vs.  $\theta$ , with a general trend toward higher fields as  $\theta$  was increased, while in the second sample these lines had a more regular angular dependence. Each sample had *one* low-field line (Figure 2) which varied sinusoidally with angle (Figure 3). A least-squares calculation of  $g$  over  $180^\circ$  yields  $g_{\parallel} = 1.136$  and  $g_{\perp} = 1.295$  for this line. (b) Many of the lines disappear (Figures 4 and 5) in more dilute (<1%) crystals, leaving but two or three prominent lines with apparent  $g_{\parallel}$  values of 1.151, 1.141, and 0.9853, all having  $g_{\perp} \sim 0$ . (c) Note especially the odd shape of the high-field line, recalling that it is the derivative mode of the spectra being presented. (d) Though the crystal is strained

(4) B. J. B. Schein, E. C. Lingafelter, and J. M. Stewart, *ibid.*, **47**, 5183 (1967).

(5) J. M. Daniels and H. Wesemeyer, *Can. J. Phys.*, **36**, 144 (1958).

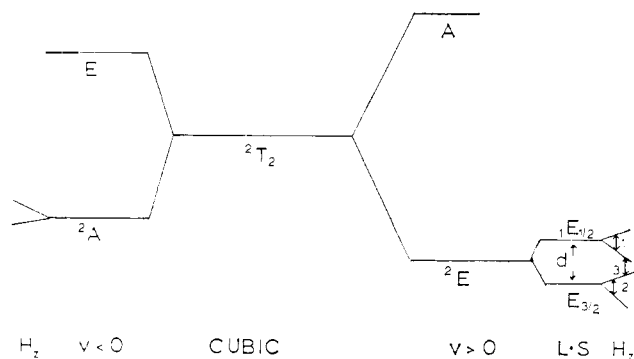


Figure 1. Ground state of  $Ti^{3+}$  in positive and negative trigonal fields.

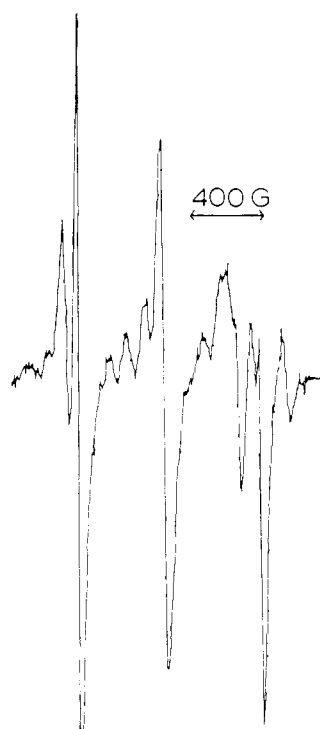


Figure 2. Epr spectrum of concentrated  $Ti^{3+}$ :GASH sample at  $4.2^\circ K$  in the 6000-G region.

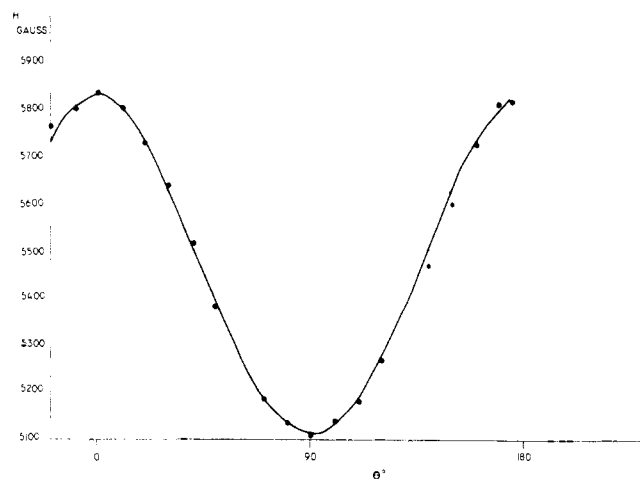


Figure 3. Rotation pattern of the low-field line of  $Ti^{3+}$ :GASH. Points are experimental, line is drawn from eq 1 with  $g_{||} = 1.136$  and  $g_{\perp} = 1.295$ .

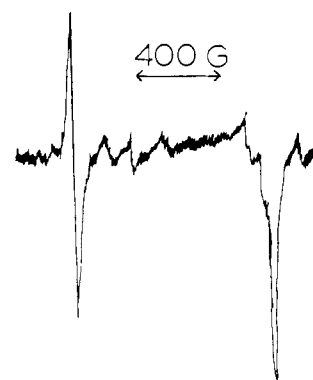


Figure 4. Detail of the same region as in Figure 2, on a dilute  $Ti^{3+}$ :GASH sample. The low-field peak (field increases to the right) is at 5843 G.

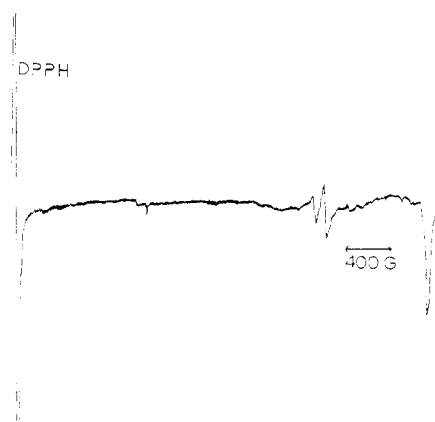


Figure 5. Epr spectrum of dilute  $Ti^{3+}$ :GGaSH.

(cf. below), the molecule retains its axial configuration as a rotation about the crystal  $c$  axis shows no change in the spectrum.

**2. Vanadium.** The trivalent ion is an  $S = 1, I = 7/2$  system and the most general spin Hamiltonian is written as

$$\mathcal{H} = \beta \mathbf{H} \cdot \mathbf{g} \cdot \mathbf{S} + \mathbf{S} \cdot \mathbf{D}' \cdot \mathbf{S} + \mathbf{S} \cdot \mathbf{T} \cdot \mathbf{I} + \mathbf{I} \cdot \mathbf{Q} \cdot \mathbf{I} \quad (2)$$

which can be written as

$$\begin{aligned} \mathcal{H} = & g_{||} \beta H_z S_z + g_{\perp} \beta (H_x S_x + H_y S_y) + \\ & D[S_z^2 - \frac{1}{3}S(S+1)] + E(S_x^2 - S_y^2) + \\ & A I_z S_z + B(I_x S_x + I_y S_y) + \\ & Q'[I_z^2 - \frac{1}{3}I(I+1)] \quad (3) \end{aligned}$$

Since  $D$  has been estimated<sup>3</sup> as  $7.2 \text{ cm}^{-1}$ , the transition observed is that between the  $m_s = \pm 1$  electronic states (Figure 6). The two problems we have been most concerned with are, first, the definition of the center of resonance as a function of angle, and second, an explanation of the unusual intensity effects we have observed.

The  $H_{\text{res}}$  vs.  $\theta$  problem can be handled in one of two ways. Suppressing the nuclear terms, the  $3 \times 3$  matrix can be diagonalized and the energy levels calculated as a function of  $\theta$  for supplied values of the parameters and  $H$ ; or a perturbation calculation can be carried out as Zverev, *et al.*, did<sup>6</sup> for  $V^{3+}$ : $Al_2O_3$ . For  $D \gg$

(6) (a) G. M. Zverev and A. M. Prokhorov, *Sov. Phys. JETP*, 11, 449 (1960); (b) G. M. Zverev and A. M. Prokhorov, *ibid.*, 13, 714 (1961).

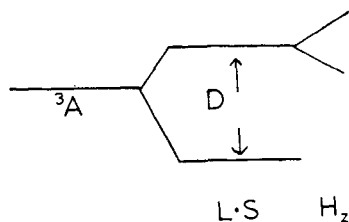


Figure 6. Ground state of trivalent vanadium, as the spin-orbit coupling and magnetic field are applied.

$g\beta H > E$  they find

$$E_{(0)} = (g_{\perp}\beta H \sin \theta)^2 / D$$

$$E_{(+1)} = D + g_{\parallel}\beta H \cos \theta + \frac{1}{2} \frac{(g_{\perp}\beta H \sin \theta)^2}{D + g_{\parallel}\beta H \cos \theta} + \frac{E^2}{2g_{\parallel}\beta H \cos \theta} + Am_I \quad (4)$$

$$E_{(-1)} = D - g_{\parallel}\beta H \cos \theta + \frac{1}{2} \frac{(g_{\perp}\beta H \sin \theta)^2}{D - g_{\parallel}\beta H \cos \theta} - \frac{E^2}{2g_{\parallel}\beta H \cos \theta} - Am_I$$

where the subscripts in parentheses are the strong-field spin quantum numbers. This approach is valid only when the spin levels do not mix. As  $\theta$  increases, the mixing increases and at a large enough angle this treatment breaks down. The energy of the observed transition, corrected from ref 6, for  $\theta \neq 90^\circ$ , is

$$E_{(+1)} - E_{(-1)} = h\nu = 2g_{\parallel}\beta H \cos \theta - \frac{(g_{\parallel}\beta H \cos \theta)(g_{\perp}\beta H \sin \theta)^2}{D^2 - (g_{\parallel}\beta H \cos \theta)^2} + \frac{E^2}{g_{\parallel}\beta H \cos \theta} + 2Am_I \quad (5)$$

which yields, for the center of resonance at  $\theta = 0^\circ$ ,  $h\nu = 2g_{\parallel}\beta H + E^2/g_{\parallel}\beta H$ , with a splitting of  $A$  between the nuclear hyperfine components. Ignoring the terms in  $B$  and  $Q'$ , these equations nicely fit the data on  $\text{Al}_2\text{O}_3:\text{V}^{3+}$ , but we found that they are not sensitive enough to  $D$  to be of use to us.

The intensity problem is also handled by a standard perturbation calculation. There is general agreement with  $\text{Al}_2\text{O}_3:\text{V}^{3+}$  in that it is predicted that all nuclear hyperfine lines ( $\Delta m_I = 0$ ) should have the same intensity and the overall intensity should increase as  $\theta$  goes from 0 to  $90^\circ$ . However, it is also predicted that only the  $\Delta m_s = \pm 2$ ,  $\Delta m_I = \pm 1$  lines should be seen at  $\theta = 0^\circ$ , which is not the case. The results do not agree with the data from  $\text{V}^{3+}:\text{GASH}$ . To explain the intensity behavior we observe, we require a spin Hamiltonian applicable when neither the Zeeman term nor the spin-spin term is diagonal. The appropriate spin Hamiltonian is presented in the Appendix.

The spectra are quite complex because of the nuclear hyperfine interaction. At least two and possibly three overlapping spectra are observed, all due to different transitions from ions on but one lattice site; *i.e.*, we assume that all occupied sites in these dilute crystals are magnetically equivalent. This is done because of the differing intensity patterns of the three spectra, as described below. The spectrum (Figure 7) consists, first, of the normal eight-line  $\Delta m_I = 0$  pattern one anticipates

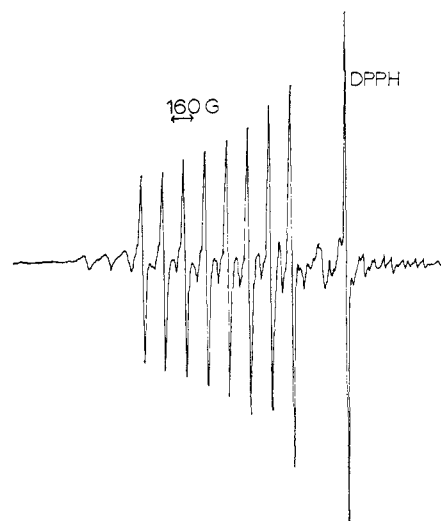


Figure 7. Epr spectrum of  $\text{V}^{3+}:\text{GASH}$  at approximately  $\theta = 30^\circ$ . (The resonances near  $g = 2$  are due to vanadyl ion.)

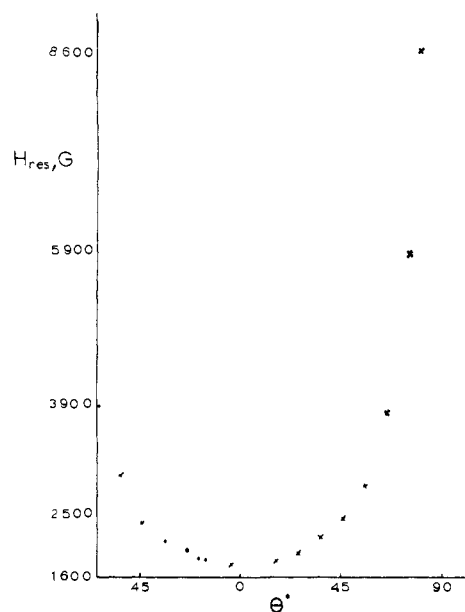


Figure 8. Center of resonance of the  $\text{V}^{3+}$  spectra as a function of angle.

from a system with nuclear spin of  $7/2$ , but the pattern is unusual, the intensity of the lines increasing to higher fields. This pattern is weak near  $\theta = 0$  and  $90^\circ$  but dominates the spectrum between 5 and  $65^\circ$ . Figure 8 illustrates the angular dependence of the center of the resonant field. Secondly, there is a seven-line spectrum due to the  $\Delta m_I = \pm 1$  transitions which lies within the eight-line pattern; this spectrum dominates at angles  $\theta$  within  $5^\circ$  of 0 and  $90^\circ$ . At angles between  $65$  and  $85^\circ$  the seven- and eight-line patterns are of comparable intensity. Figure 9 illustrates the two spectra at high gain near  $\theta = 0^\circ$ , where the greater intensity of the seven-line pattern is clear, as well as the different intensity features of the two spectra, the seven-line one peaking in the middle. It is because of the very different intensity behavior with respect to  $\theta$ , as well as the center of the spectrum, that we do not assign the different spectra to the two magnetically inequivalent sites

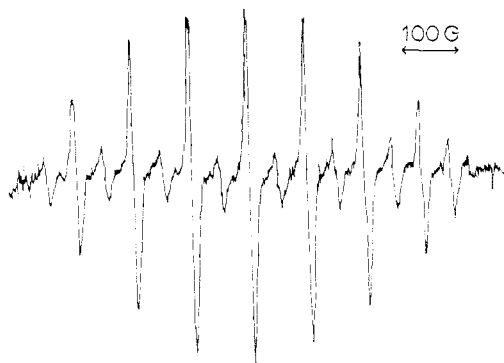


Figure 9. Epr spectrum of  $V^{3+}$ :GASH at approximately  $\theta = 0^\circ$ .

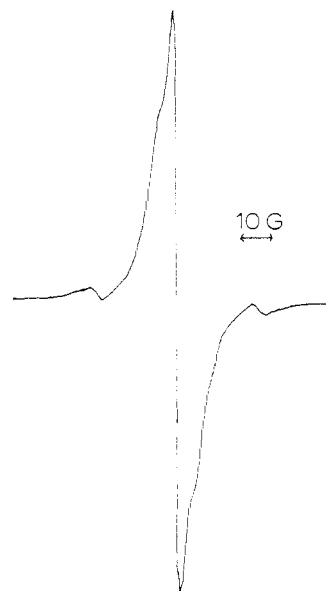


Figure 10. Detail of the  $1/2 \leftrightarrow -1/2$  transition of  $Cr^{3+}$ :GASH at  $\theta = 0^\circ$  at ambient temperatures. The satellites are assigned to the  $^{53}Cr$  hyperfine structure.

in the lattice. The lack of resolution of the  $\Delta m_I = \pm 1$  lines into two shows that the quadrupole term ( $Q'$ ) is less than the line width, which at  $\theta \sim 50^\circ$  is less than 40 G. Lastly, Figure 7 shows a spectrum at  $\theta = 30^\circ$  with three lines at the low-field side of the main spectrum clearly discernible. There are also three similar lines on the high-field side, but they are masked at this orientation by the overlapping vanadyl spectrum. The lines are of equal intensity and may be part of a larger spectrum, the remaining lines being situated between the eight principal lines. This is usually the weakest pattern in the spectrum. At angles  $< 65^\circ$ , the splitting between adjacent lines in any one of the three spectra is the same. At any given angle this splitting is the same in all three spectra, and all spectra have the same center of resonance. The lines broaden as  $\theta$  increases and the separation between the hyperfine components increases until about  $85^\circ$ , above which it begins to decrease until at  $\theta = 90^\circ$  only one broad ( $\sim 1000$  G) line is observed at about 12,000 G, and about 1000 times the intensity at  $\theta = 0^\circ$ . Similar behavior was also observed for  $V^{3+}$  in corundum, and was ascribed to microdomains with slightly different axial directions.<sup>6</sup>

**3. Chromium.** The main features of the epr spectrum of trivalent chromium ( $S = 3/2$ ) in GASH and its

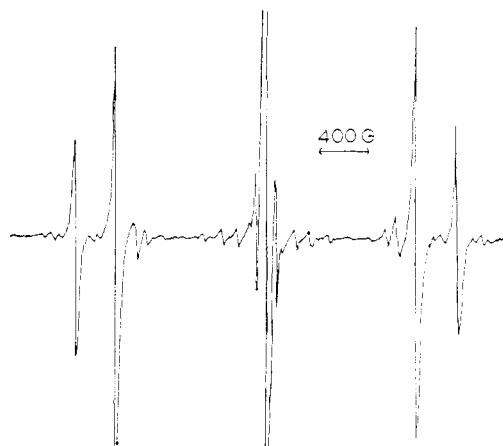


Figure 11. Epr spectrum of concentrated  $Cr^{3+}$ :GASH at  $\theta = 0^\circ$  and ambient temperature.

isomorphs have been reported earlier,<sup>5,7,8</sup> and our results agree. The spectra clearly illustrate the magnetic inequivalence of the two sites in GASH for small ions, with slightly different values of  $g$  and  $D$ . A portion of the spectrum, that near the  $-1/2 \leftrightarrow 1/2$  transition at  $\theta = 0^\circ$  in a dilute crystal, is illustrated in Figure 10. The lines indicated are assigned as the previously unreported nuclear hyperfine splitting from the 9.54% abundant  $^{53}Cr$ , with  $I = 3/2$ . The relative intensities and splittings are similar to such transitions in other systems.<sup>9</sup> These lines can also be seen flanking the  $\pm 3/2 \leftrightarrow \pm 1/2$  transitions at  $\theta = 0^\circ$ , but as  $\theta$  varies from this angle other lines (*cf.* below) appear and it becomes difficult to assign the nuclear hyperfine lines. We find  $A_z \sim 16$  G in both GASH and its deuterio isomorph.

Dilute ( $< 1\%$ ) samples under moderately high gain and concentrated (5%) samples at low gain exhibit many extra lines in the spectrum of  $Cr^{3+}$  that cannot be explained by either fine-structure ( $D$ ,  $E$ ) or hyperfine-structure terms in the spin Hamiltonian. It was found that the relative intensity of these lines compared to the electronic transitions increased with increasing chromium concentration. The lines, illustrated in Figure 11, are assigned as being due to magnetic exchange between  $Cr^{3+}$  ions which have clustered in the crystal. A portion of the spectrum at a constant  $\theta = 90^\circ$  but with rotation about the  $z$  (or  $c$ ) axis is shown in Figure 12, where it can be seen that the lines change position and intensity with a  $60^\circ$  periodicity.

**4. Manganese.** We have observed a spectrum due to  $Mn^{3+}$  in GGaSH at 4.2°K but it is so complicated that we have not yet been able to unravel it. The fact that no spectrum is observed at either room temperature or 77°K shows that it is not due to divalent manganese. The complexity of the spectrum arises because there appear to be several sites. This, coupled with the numerous nuclear hyperfine- ( $I = 5/2$ ) and fine-structure ( $S = 2$ ) transitions, give a complex spectrum.

**5. Iron.** The spectrum has been reported earlier at room and liquid nitrogen temperatures,<sup>10</sup> and our results are in agreement. We find a decrease in the rela-

(7) G. Burns, *Phys. Rev.*, **123**, 1634 (1961).

(8) G. S. Bogle, J. R. Gabriel, and G. A. Bottomly, *Trans. Faraday Soc.*, **53**, 1058 (1957).

(9) W. Low, *Phys. Rev.*, **105**, 801 (1957).

(10) E. G. Brock, D. Stirpe, and E. I. Hormats, *J. Chem. Phys.*, **37**, 2735 (1962).

tive intensity of the higher field transitions at 4.2°, showing that  $D$  is negative. Samples examined at 4.2°K exhibit a wealth of superhyperfine structure on the fine-structure lines, a subject that we shall take up in a future publication.

**6. Vanadyl.** The spectrum of  $\text{VO}^{2+}$  with  $g$  close to 2 has been observed in all GASH crystals which also contain  $\text{V}(\text{H}_2\text{O})_6^{3+}$ . We have not examined these spectra carefully, for the spectrum of hydrated vanadyl ion is well known,<sup>11,12</sup> but it is relevant to our discussion below that the GASH host readily accepts the large divalent vanadyl ion.

## Discussion

The most striking feature of the epr spectrum of trivalent titanium in GASH and its isomorphs is the large number of lines observed. We address ourselves primarily to this question, keeping in mind the hint offered by the polarized optical spectrum, namely that the bands are *not* strongly polarized. This would be a natural consequence if the trigonal field is not large.

Ignoring nuclear hyperfine structure, which we have not observed, one expects but one line for each magnetic site in the epr spectrum of titanium in a trigonal field, irrespective of the sign of  $v$ .<sup>13</sup> Such is the case experimentally for such hosts as  $\text{Al}_2\text{O}_3$ ,<sup>14</sup>  $\text{AlCl}_3 \cdot 6\text{H}_2\text{O}$ ,<sup>15</sup> aluminum acetylacetonate,<sup>16</sup> as well as several others.<sup>17</sup> The spectrum displayed in Figure 2 must then be assigned, at least in part, to titanium ions on a variety of lattice sites. This is not unreasonable, for the ion is half again as large as the aluminum host which it replaces; furthermore, three complexes have been reported for titanium in cesium alum,<sup>18</sup> a host lattice not unlike that of GASH. What is interesting here is that the 2:1 site symmetry of the host lattice, illustrated so nicely by the chromium ion, is substantially lost when titanium is the guest. In fact, we suggest that titanium enters the lattice in a random fashion, creating impurity defects as distinct from isomorphous replacement.

This postulate is given added weight when we analyze the  $g$  values, and we consider first the line with  $g_{\parallel} = 1.136$  and  $g_{\perp} = 1.295$ . McGarvey<sup>13</sup> has shown that these  $g$  values are consistent with an A ground state ( $v < 0$ ), and  $v$  can be estimated from the equations

$$g_{\parallel} = 2.0023 \cos 2\gamma - 2(2a^2 - b^2) \sin^2 \gamma + (18a^2b^2 \sin^2 \gamma + 3\sqrt{6}a^2b \sin 2\gamma)\epsilon \quad (6)$$

$$g_{\perp} = 2.0023 \cos^2 \gamma - \sqrt{6}b \sin 2\gamma - (6a^2 \cos^2 \gamma + \frac{3}{2}\sqrt{6}a^2b \sin 2\gamma)\epsilon$$

$$\tan 2\gamma = \sqrt{6}b\eta[1 + \frac{1}{2}(2a - b^2)\eta]^{-1}$$

where  $\epsilon = \zeta/10Dq$ ,  $\zeta$  is the spin-orbit coupling constant,  $\eta = \zeta/v$ , and  $a$  and  $b$  are geometric factors which may take the values  $a^2 = 2/3$  and  $b^2 = 1/3$  for a small distortion of an octahedron. Taking a reasonable value for

- (11) R. H. Borcherts and C. Kikuchi, *J. Chem. Phys.*, **40**, 2270 (1964).  
 (12) K. V. S. Rao, M. D. Sastry, and P. Venkateswarlu, *ibid.*, **49**, 4984 (1968).  
 (13) B. R. McGarvey, *Transition Metal Chem.*, **3**, 89 (1966).  
 (14) L. S. Kornienko and A. M. Prokhorov, *Sov. Phys. JETP*, **11**, 1189 (1960).  
 (15) E. Y. Wong, *J. Chem. Phys.*, **32**, 598 (1960).  
 (16) B. R. McGarvey, *ibid.*, **38**, 388 (1963).  
 (17) H. M. Gladney and J. D. Swalen, *ibid.*, **42**, 1999 (1965).  
 (18) G. A. Wootton and J. A. MacKinnon, *Can. J. Phys.*, **46**, 59 (1968).

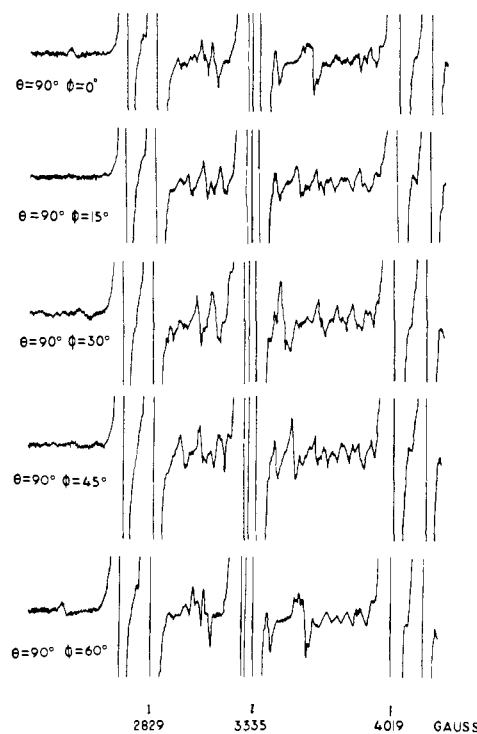


Figure 12. Rotational pattern of the extra lines in the  $\text{Cr}^{3+}$  spectra as  $\theta$  is held constant but rotation is carried out along the  $c$  axis. The 60° rotational symmetry is illustrated.

$\zeta$  (80% of the free-ion value) the experimental  $g$  values may be fit by the above equations with  $v$  of the order of  $-100$  to  $-300 \text{ cm}^{-1}$ . While the calculation is not exact, it is clear that a measurable fraction of the titanium ions present has an orbital singlet ground state and a fairly small trigonal field. (Dionne<sup>19</sup> offers an alternative procedure for calculating  $v$  from the  $g$  values, and we use it to find  $v \sim -300$  to  $-400 \text{ cm}^{-1}$ , consistent with the above calculation.)

*The remainder of the spectrum must be assigned to ions with positive  $v$ , that is, the orbital doublet is the ground state.* This is because the  $g$  values are very anisotropic, with  $g_{\parallel}$  being about one, and  $g_{\perp}$  approaching zero. These result when  $v < 0$ , as has been discussed by Gladney and Swalen.<sup>17</sup> The situation resembles  $\text{Ti}^{3+}:\text{Al}_2\text{O}_3$ , for which  $g_{\parallel} = 1.067$ ,  $g_{\perp} < 0.1$ , and where direct measurement in the far-infrared has confirmed the ground-state assignment<sup>20,21</sup> and shown that the splitting between  ${}^2E_{1/2}$  and  $E_{3/2}$  is only  $+107 \text{ cm}^{-1}$ . While we cannot estimate  $v$  here, we do propose a mean value for  $d$  (Figure 1), which has been shown to be  $37.8 \text{ cm}^{-1}$  in  $\text{Ti}^{3+}:\text{Al}_2\text{O}_3$ .<sup>20,21</sup> Our assignment is based on the odd-shaped high-field line illustrated in Figure 4. The apparent  $g$  value is small and the unusual shape of the line suggests a resonance mechanism for this line which differs from that for the other lines. Low and Weger<sup>22</sup> observed a line of similar shape in the spectrum of  $\text{Fe}^{2+}:\text{MgO}$ , and calculations by McMahon<sup>23a</sup> suggest that strain in the crystal is responsible

- (19) G. F. Dionne, *Phys. Rev. A*, **137**, 743 (1965).  
 (20) R. M. Macfarlane, J. Y. Wong, and M. D. Sturge, *ibid.*, **166**, 250 (1968).  
 (21) R. R. Joyce and P. L. Richards, *ibid.*, **179**, 375 (1969).  
 (22) W. Low and M. Weger, *ibid.*, **118**, 1130 (1969).  
 (23) (a) D. H. McMahon, *ibid.*, **A**, **134**, 128 (1963); (b) S. A. Altshuler, Sh. Sh. Bashkurov, and M. M. Azripov, *Sov. Phys. Solid State*, **4**, 2465 (1963).

for the spin relaxation and consequent line shape. Since we have already shown that titanium enters the GASH lattice in an unusual fashion, it is very reasonable to suggest that strain likewise contributes to the unusual features here.

But consider an additional proposal. Suppose the prominent lines (1 and 2) in the spectrum are assigned not to separate ions but to transitions within the two Kramer's doublets coming from the trigonal  ${}^2E$  state. After obtaining the  $g$  values for the two lines, we note that the equation for resonance between the  $m_s = +1/2$  state of the lower doublet and the  $m_s = -1/2$  state of the upper doublet is

$$h\nu = -1/2g_1\beta H_3 - 1/2g_2\beta H_3 + d \quad (7)$$

Using this equation we have been able to fit nicely the resonant field of the anomalous line at six different angles with  $d = 0.660 \pm 0.002 \text{ cm}^{-1}$ . Such an assignment of a  $\Delta m_s = \pm 1$  transition between two different Kramer's doublets explains the anomalously low  $g$  value as well as its shape, as we might expect a different relaxation mechanism for such a transition.

(Only one line, also odd shaped, has been reported for the spectrum of  $\text{Ti}^{3+}:\text{Al}_2\text{O}_3$ , and it has been assigned to the normal Kramer's transition. While Altshuler, *et al.*,<sup>23b</sup> have suggested that the shape is due to a distribution of different rhombic distortions (*i.e.*, strain), we justify our assignment to the non-Kramer's transition because, first, we have other lines that appear to be the normal Kramer's transitions; secondly, the  $g$  value of this line is much smaller, and thirdly, our assignment can be fitted nicely at six different angles.)

The fact that vanadyl ions can enter the hydrogen-bonded GASH lattice suggests that the spatial restrictions on titanium will not be large, and that the octahedron of water molecules around the  $\text{M}^{3+}$  sites is readily deformed. This, plus the evidence for clustering by  $\text{Cr}^{3+}$  discussed below, leads us to propose the following situation for titanium. An isolated ion entering the lattice distorts the crystal locally. A second ion, entering at a nearest neighbor position would then be in a site distorted not only by its own presence but by the initial titanium as well. The number of sites is also increased by the magnetic inequivalence of the sites of the host lattice. A third titanium entering as a nearest neighbor to either of the other ions could be in a different environment, with the number of possible sites increasing geometrically with the number of nearest neighbors. Should the distortion at any position in the lattice be large, even second nearest neighbor positions would be affected. These factors would cause enough of a variety of sites that titanium ions would experience not only different crystal-field strengths but even different signs of the trigonal field. This behavior is consistent with the lack of strong polarization of the optical spectra<sup>2</sup> and yields a small trigonal splitting.

Results in  $\text{GGaSH}$ , where the  $\text{Ga}^{3+}$  is slightly larger than  $\text{Al}^{3+}$ , support the replacement hypothesis, as only the three lines associated with the  ${}^2E$  ground state have been observed.

The only earlier example of epr of trivalent vanadium concerns that of  $\text{V}^{3+}$  in corundum, although  $\text{V}^{3+}$  has recently been investigated in  $\text{MgO}$  by acoustic paramagnetic resonance.<sup>24</sup> The large zero-field splitting

requires<sup>25</sup> large, pulsed magnetic fields in order to observe the  $\Delta m_s = \pm 1$  transition, but the  $\Delta m_s = \pm 2$  transition is easily observed<sup>6,26</sup> at X-band. The best available parameters are  $g_{\parallel} = 1.915$ ,<sup>6</sup>  $g_{\perp} = 1.744$ ,<sup>27</sup>  $D = 7.97 \text{ cm}^{-1}$ , and  $E < 10^{-2} \text{ cm}^{-1}$ .<sup>6</sup> The hyperfine splitting constant is  $A = 110 \text{ G}$ .<sup>26</sup> The intensity of the transition is low at  $\theta = 0^\circ$  and increases with increasing angle, *the hyperfine components are of equal intensity*, and only the  $\Delta m_I = 0$  transitions have been observed. We have confirmed these latter observations on a crystal loaned to us by Professor D. S. McClure.<sup>23</sup> Furthermore, at  $\theta > 70^\circ$ , the resonance becomes very broad, and the hyperfine components are not resolved.

The spectrum of  $\text{V}^{3+}$  in GASH is quite different from that of  $\text{V}^{3+}$  in  $\text{Al}_2\text{O}_3$ , although the ion experiences a trigonal field in both cases. Since the zero-field splitting is large, the  $\Delta m_s = \pm 2$  transition is the one of concern. The spectrum can be obtained only at liquid helium temperatures.

The most obvious feature of the spectrum is the appearance of at least two and perhaps three sets of overlapping resonances with different intensities. In order to present a convincing argument for our assignments, we have carried out perturbation calculations of expected intensity patterns, using the spin Hamiltonian in the Appendix. These have been carried out in the usual fashion, by calculating  $[\langle -1, m_I | S_x | +1, m_I \rangle]^2$  and  $[\langle -1, m_I | S_y | +1, m_I \pm 1 \rangle]^2$ , where the prime denotes a wave function corrected to first order.

A  $\Delta m_s = \pm 1, \Delta m_I = 0$  transition usually has maximum intensity at  $\theta = 0^\circ$ , but since we are dealing with a  $\Delta m_s = \pm 2$  transition, we calculate that  $\Delta m_I = 0$  (usual allowed nuclear) transition has zero intensity at  $\theta = 0$  and  $90^\circ$ , and this is indeed what we find for the eight-line pattern. The seven-line pattern is the predominant one at  $\theta = 0^\circ$ , and we calculate that the intensity should go as  $[I(I+1) - m_I(m_I+1)]$ , giving relative intensities of 14:24:30:31:30:24:14. We observe relative intensities (peak-to-peak heights) of approximately 14:24:29.3:33.1:29.3:24.6:14, which is fairly good agreement, since the spectra are extremely sensitive to angle at low angles and the crystal could be easily misaligned a degree.

At angles intermediate between 0 and  $90^\circ$ , the intensity formula for the  $\Delta m_I = 0$  transitions takes the form  $\alpha + \beta m_I + \gamma m_I^2$ , which predicts increasing intensity to higher field for negative  $A$  (or  $A_{\parallel}$ ) and  $B$  (or  $A_{\perp}$ ). This also agrees well with experiment, as can be seen in Figure 7. The measured intensities for  $45^\circ < \theta < 55^\circ$  have been found to be 46:48:51:53:55.5:61:65:73.5, and on another sample at  $\theta = 16^\circ$ , 9.5:11:12:12.5:12:14.5:15:17.8. The  $\Delta m_I = \pm 1$  lines go as  $C_1[I(I+1) - m_I(m_I-1)] + C_2[I(I+1) - m_I(m_I+1)]$ , which predicts a peaking of intensity near the middle of the spectrum. We find, again for  $45^\circ < \theta < 55^\circ$ , the experimental intensities going as 2:3:5:7.5:9:8:8, in fair agreement. At intermediate angles the intensity

(24) R. G. Brabin-Smith and V. W. Rampton, *Proc. Phys. Soc., London (Solid State Phys.)*, **2**, 1759 (1969).

(25) S. Foner and W. Low, *Phys. Rev.*, **120**, 1585 (1960).

(26) J. Lambe and C. Kikuchi, *ibid.*, **118**, 71 (1959).

(27) A. R. Smith and R. W. Mires, *ibid.*, **172**, 265 (1968).

(28) In this particular crystal the  $\text{V}^{3+}$  transitions have a distorted line shape very similar to that for  $\text{Ti}^{3+}$  in  $\text{Al}_2\text{O}_3$ . Another resonance, probably  $\text{Fe}^{3+}$ , is also seen in this crystal, but its line shape is normal. This is further evidence that the size of the dopant is of great importance. Here the large  $\text{V}^{3+}$  shows strain effects while  $\text{Fe}^{3+}$  does not.

pattern cannot be measured exactly due to apparent overlap with a third spectrum.

At  $\theta$  of  $90^\circ$ , one calculates that the  $\Delta m_I = 0$  lines again have zero intensity, but the  $\pm 1$  lines should go as  $[I(I+1) - m_I^2 - m_L]$ , which suggests that the lines of maximum intensity should now lie to the low-field end of the spectrum, and we have indeed found this intensity pattern very close to  $\theta = 90^\circ$ .

Three broad lines to both low field and high field of the main spectrum have always been observed for  $V^{3+}$ :GASH, but the overlapping lines in the principal spectrum have prevented us from determining without question whether they alone form a complete resonance pattern or belong to, say, a 13-line, overlapping spectrum. This resonance has not been observed for  $V^{3+}$  in GGaSH, a crystal in which we have seen the other spectral features reported here. The lines might be due to interactions, either exchange or dipolar, between the magnetic ions in GASH, while the particular  $V^{3+}$ :GGaSH crystals we studied might have been too dilute to exhibit the extra lines.

Implicit in the preceding discussion has been our assumption of only one type of  $V^{3+}$  site in GASH and GGaSH, and that this is due to size effects. Pure crystals of GVSH are easily grown, indicating that  $V^{3+}$  can enter both sites; therefore, we propose that while the  $V^{3+}$  may enter both lattice sites in the host crystals, its larger size causes them to be magnetically equivalent. Confirmation of this awaits the determination of the crystal structure of GVSH,  $C(NH_2)_3V(SO_4)_2 \cdot 6H_2O$ . Should our hypothesis not be confirmed, we would then have to conclude that  $V^{3+}$  enters preferentially one of the lattice sites and enters the second when concentration effects force it to.

We find  $A \sim 102$  G directly from the splitting at  $\theta$  of  $0^\circ$ . The parameter  $D$  has been used as reported earlier,  $7.2 \text{ cm}^{-1}$ , but without diagonalizing the  $24 \times 24$  matrix as a function of angle we are left with four other parameters,  $B$ ,  $E$ ,  $g_{\parallel}$ , and  $g_{\perp}$ , and two pieces of data, namely those angles ( $0, 90^\circ$ ) where the matrix can be solved analytically. Since the transition at  $\theta = 0^\circ$  is at almost the same field as that of  $V^{3+}$  in  $Al_2O_3$ , we assume with Prokhorov and Zverev that  $E \ll g\beta H$ . The parameter  $E$  cannot be very large, otherwise we would not observe the resonance at such low fields ( $1800$  G at  $\theta = 0^\circ$ ). In a perturbation calculation  $E$  enters as  $E^2/g\beta H$  so an  $E$  as large as  $0.1 \text{ cm}^{-1}$  would not have a noticeable effect on the value of  $g_{\parallel}$ . However, even for titanium, which appears to cause a larger distortion of the lattice than does vanadium, the symmetry appears to be axial as determined by a rotation about the  $c$  axis. Measurements at another frequency would give us two pieces of data for the two unknowns at  $\theta = 0^\circ$ . Thus we have carried out all perturbation calculations assuming  $E$  is zero and have calculated  $g_{\parallel} = 1.86$  for  $V^{3+}$ :GASH, which is quite similar to that reported for  $V^{3+}$ : $Al_2O_3$ . The parameter  $g_{\perp}$  cannot be taken directly from the spectrum at  $\theta = 90^\circ$  because, as noted above, the absorption is quite broad. The maximum field of resonance of  $12,000$  G however, may be compared with that for corundum,  $20,000$  G, suggesting that  $g_{\perp}$  (GASH)  $> g_{\perp}$  ( $Al_2O_3$ ).

If we were to use eq 4 above for our calculation of  $g_{\perp}$ , a value of  $2.6$  would be obtained. This seems anomalously large and suggests that either the equations are

not valid or that  $D$  is smaller than previously determined. This result, coupled with the fact that the zero-field splitting does not seem to determine the axis of quantization, suggests that  $D$  may not be as large as the  $7.2 \text{ cm}^{-1}$  suggested earlier; in fact, if we accept  $2.0$  as an upper limit for  $g_{\perp}$ , then using eq 4 of ref 6b

$$D = (g_{\perp}\beta H)^2/h\nu \quad (8)$$

we calculate a  $D$  of only about  $3.8 \text{ cm}^{-1}$ . This would still be large enough, of course, to prevent the observation of the usual  $\Delta m_s = \pm 1$  transition.<sup>28a</sup>

We turn now to a discussion of the chromium spectra, the main features of which are already clear.<sup>6,7,8</sup> The nuclear hyperfine splitting constant observed is of similar magnitude to that reported in 15 other host lattices<sup>29</sup> and requires no further comment. The ion enters the GASH lattice by isomorphous replacement, a reflection of the fact that it is close in size to the aluminum ion it replaces. The most interesting aspect of our results is the proof that the myriad of weak lines is due to magnetic exchange between two or more chromium ions. We have tried to fit the spectrum to a term of the form  $\mathcal{H} = -2JS_1 \cdot S_2$  in the spin Hamiltonian, but this requires an assignment of each line to a specific site: nearest neighbors, next-nearest neighbors, triplets, and so on. We have not found such an unambiguous assignment.

Since chromium is well known to cluster at low concentrations in other lattices,<sup>30</sup> it comes as no surprise that it happens in GASH as well. What is interesting is that the effect is observable, for we note the following facts from the crystal structure.<sup>4</sup> The distance between closest ions is  $6.777 \text{ \AA}$ , a distance too large for direct exchange. The superexchange mechanism must be operative, but the path must be tortuous, for there are no bridging ligands. Rather, each ion is in the usual octahedron of water molecules, and the path must involve at least two water molecules in the hydrogen-bonded lattice. Recent experiments have shown that deuteration affects the magnetic phase diagram of hydrated metal ions, clearly showing that the superexchange effect is long range.<sup>31</sup>

Furthermore, looking down the trigonal axis of the crystal, one notes that each metal ion has six nearest neighbors, three above it and three below, arranged in sixfold symmetry about the reference ion for a projection onto the plane perpendicular to  $c$ . A crystal was mounted with the  $c$  axis normal to the magnetic field which should effectively cause such a projection, and the spectrum recorded every  $15^\circ$  ( $\theta$  is constant but  $\phi$  varies). As Figure 12 illustrates, the fine-structure lines remain constant, while the lines assigned to magnetic exchange do indeed exhibit sixfold rotational symmetry. This evidence, combined with the fact that the intensity of these lines relative to the electronic lines is a function of concentration, confirms the identification. Furthermore, this tends to confirm the earlier assignment<sup>1</sup> of

(28a) NOTE ADDED IN PROOF. Measurement of  $\chi_{\parallel}$  and  $\chi_{\perp}$  of GVSH between  $1.5$  and  $20^\circ\text{K}$  shows that  $g_{\perp} = 1.66$  and  $D = 3.74 \text{ cm}^{-1}$ : J. H. McElearney, R. W. Schwartz, S. Merchant, and R. L. Carlin, submitted for publication.

(29) B. R. McGarvey, *J. Phys. Chem.*, **71**, 51 (1967).

(30) J. Owen, *J. Appl. Phys.*, **32**, 2135 (1961).

(31) H. Forst, P. T. Bailey, and J. R. Ricks, *Phys. Lett. A*, **30**, 52 (1969), and references therein.

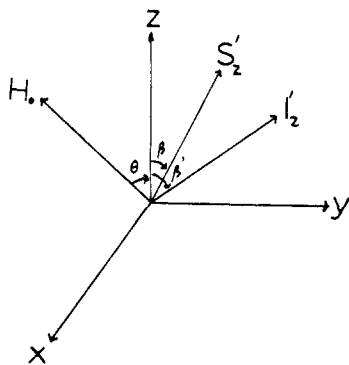


Figure 13. Orientation of the axes of electron spin quantization ( $S'_z$ ) and the nuclear spin quantization ( $I'_z$ ) with respect to the crystal coordinate system when the magnetic field makes an angle  $\theta$  with respect to the  $z$  axis of the molecule.

many of the sharp lines in the optical spectrum of undiluted GCrSH to magnetic exchange.

**General Conclusions.** The GASH system is unique. Though this is merely a tautology, the effects that we have found in this lattice are most unusual, and unlike those reported in any other *single* lattice. This is due in part to the fact that there are relatively few systems in which a wide variety of trivalent iron series ions have been examined, all in one host. Corundum, of course, is one host that has been studied even more extensively, and we made several comparisons above with studies of the epr spectra of ions in this host.

We feel that the predominant factor affecting the electronic structure of metal ion guests in GASH is simply that of size, a point we have made repeatedly already. We find the effect fascinating since, as we pointed out previously,<sup>1,2</sup> the GASH lattice is a rather open, hydrogen-bonded one. One might have anticipated that the system, which easily accepts many different transition metal ions over a wide concentration range, would do so with a minimum of stress and strain. That this is not so is clear from our results as detailed above. Yet when considering strain on a microscopic level one concludes that it involves the displacement of neighbors. So, GASH should show strain in a different way than  $\text{Al}_2\text{O}_3$ , where nuclear motion is rather restricted and the doubly charged oxygen ions cannot move a great deal. Hence, basically one site is found with  $\text{Ti}^{3+}:\text{Al}_2\text{O}_3$ , and many with  $\text{Ti}^{3+}:\text{GASH}$ ;  $\text{V}^{3+}:\text{Al}_2\text{O}_3$  shows much the same strain as  $\text{Ti}^{3+}:\text{Al}_2\text{O}_3$ , while  $\text{V}^{3+}:\text{GASH}$  "relieves" this strain by occupying only one site. Also, consider the difference in values of  $d$  for  $\text{Ti}^{3+}$  in  $\text{Al}_2\text{O}_3$  and GASH. A dynamic Jahn-Teller effect quenches<sup>20</sup> the spin-orbit coupling, causing  $d$  to take a smaller value than one calculates using crystal-field theory. This effect appears to be more pronounced in GASH, where  $d$  is smaller by almost two orders of magnitude. All of the above can be considered a consequence of the discrete, nonrigid  $\text{M}(\text{H}_2\text{O})_6^{3+}$  complex, compared to corundum, where no separate  $\text{AlO}_6$  units exists.

The vanadium case is of interest because, even though  $D$  is still much greater than  $g\beta H$ , the effect of the magnetic field is seen to shift the axis of quantization. We intend to remeasure  $D$  and  $g_{\perp}$  directly from the paramagnetic anisotropy of the crystals at low temperatures.

**Acknowledgment.** Acknowledgment is made to the donors of the Petroleum Research Fund, administered by the American Chemical Society, for partial support of this research. Two research grants from the National Science Foundation have also provided important support. R. W. S. has been a University of Illinois Fellow, 1968–1970. We have profited from conversations with Dr. Robert N. Schwartz, and Bruce Spivack assisted with some of the experimental work.

## Appendix

The most general form of a spin Hamiltonian for a transition metal ion ( $S < 2$ ) was given as eq 2 of the main text, except that a nuclear Zeeman term was omitted because we found no evidence for it here. The procedure for obtaining a spin Hamiltonian useful for the reduction of experimental data has been sketched out by Orton<sup>32</sup> and given in more detail by Weaver,<sup>33</sup> Further details of our calculation are also available.<sup>34</sup>

One usually finds either the electronic Zeeman or dipolar spin-spin term as the largest term in the spin Hamiltonian. Diagonalizing this largest term specifies that the electron spin is quantized along some axis making an angle  $\beta$  with the symmetry axis. This ensures that the largest interaction in  $\mathcal{H}$  will have terms involving  $S_z$ , present, *i.e.*, that no off-diagonal elements exist. This is accomplished by a suitable rotation of the spin operators.

The nuclear spin terms are treated analogously. The treatment of the hyperfine interaction is particularly dependent on the use to which  $\mathcal{H}$  will be put. Usually the coefficients of all terms which mix nuclear levels of the same electronic level are set equal to zero so that perturbation calculations can be carried out.

For  $\text{V}^{3+}:\text{GASH}$  we find neither of the two forms of  $\mathcal{H}$  in general use will explain our data. It is known from this and previous work that  $D \gg g\beta H$ , yet the spin Hamiltonian written in this approximation gives incorrect predictions for the intensities, even when the wave functions are corrected to second order. While the form of  $\mathcal{H}$  derived when  $D \ll g\beta H$  does predict the correct intensities, we know that this condition is not met in our system. The procedure for finding an  $\mathcal{H}$  intermediate between these two is described below.

We first write the spin Hamiltonian for  $D \gg g\beta H$ , leaving out the rhombic ( $E$ ) and quadrupole ( $Q'$ ) terms, which are not required here.

$$\mathcal{H} = D[S_z^2 - \frac{1}{3}S(S+1)] + g_{\parallel}\beta H \cos \theta S_z + g_{\perp}\beta H \sin \theta S_x + A(I_z S_z) + B(I_x S_x + I_y S_y)$$

This quantizes the electron spin along the symmetry or  $z$  axis as well as diagonalizing the spin-spin term. Because the system is axial we choose the  $x$  axis to be in the plane of  $\mathbf{H}$  and the  $z$  axis<sup>13</sup> and this eliminates  $S_y$  from the Zeeman term. Referring to Figure 13, we rotate this  $\mathcal{H}$  to the coordinate frame where both electron and nuclear spins are actually quantized, by an Euler transformation of  $S_x$ ,  $S_y$ , and  $S_z$ , and of  $I_x$ ,  $I_y$ , and  $I_z$ , to

(32) J. W. Orton, "Electron Paramagnetic Resonance," Illife Books, London, 1968, Chapter 4.

(33) H. Weaver, Seventh Annual Nmr-Epr Workshop, Varian Associates, Palo Alto, Calif., 1963.

(34) R. W. Schwartz, Ph.D. Thesis, University of Illinois at Chicago Circle.



the primed coordinate system. The angles  $\beta$  and  $\beta'$  will depend on  $\theta$  in some fashion. Using a standard Euler matrix,<sup>35</sup> and allowing the arbitrary angle  $\alpha$  to be 0, we have

$$\begin{aligned} S_x &= S_{x'} \cos \beta - S_{z'} \sin \beta \\ S_y &= S_{y'} \\ S_z &= S_{z'} \sin \beta + S_{x'} \cos \beta \end{aligned}$$

where we have assumed axial symmetry. The angle  $\gamma$  is then arbitrary and we have set it equal to  $0^\circ$ . The expressions for  $I_x$ ,  $I_y$ , and  $I_z$  may be obtained by replacing the  $S$ 's by  $I$ 's, and  $\beta$  by  $\beta'$ . The spin Hamiltonian then becomes

$$\begin{aligned} \mathcal{H} &= \beta H_0 \{ (g_{\parallel} \cos \theta \cos \beta - g_{\perp} \sin \theta \sin \beta) S_{z'} + \\ &\quad (g_{\parallel} \cos \theta \sin \beta + g_{\perp} \sin \theta \cos \beta) S_{x'} \} + \\ &\quad (D/2) \{ [S_{z'}^2 - \frac{1}{3} S(S+1)] \cos^2 \beta + \\ &\quad \frac{(S_{+'}^2 + S_{-'}^2)}{2} \sin^2 \beta + [(S_{+'} + S_{-'}) S_{z'} + \\ &\quad S_{z'}(S_{+'} + S_{-'}) \sin \beta \cos \beta \} + [A_{\parallel} \sin \beta \sin \beta' + \\ &\quad A_{\parallel} \cos \beta \cos \beta'] S_{z'} I_{z'} + [A_{\parallel} \sin \beta \sin \beta' + \\ &\quad A_{\perp} (\cos \beta \cos \beta' - 1)] \frac{(S_{+} I_{+} + S_{-} I_{-})}{4} + \end{aligned}$$

(35) M. E. Rose, "Elementary Theory of Angular Momentum," Wiley, New York, N. Y., 1957, p 65.

$$\begin{aligned} &[A_{\parallel} \sin \beta \sin \beta' + A_{\perp} (\cos \beta \cos \beta' + 1)] \times \\ &\quad \frac{(S_{+} I_{-} + S_{-} I_{+})}{4} + (A_{\parallel} \cos \beta' \sin \beta' - \\ &\quad A_{\perp} \sin \beta' \cos \beta') [(S_{+} + S_{-}) I_{z'}] \end{aligned}$$

by making the usual substitution of raising and lowering operators for  $x$  and  $y$  operators. One additional constraint we have applied is that the coefficient of the term in  $S_{z'} I_{z'}$  should be zero, as previously mentioned. This condition leads to a relationship between  $\beta$  and  $\beta'$ , namely  $A \tan \beta' = B \tan \beta$ , but no general expression is available to relate  $\theta$  to  $\beta$  or  $\beta'$ .

The spin Hamiltonian derived in this way is almost of the same form as that found when  $D \ll g\beta H$ . One difference is the additional term in  $S_{z'}$  in the Zeeman interaction, but this does not affect the form of the perturbed wave functions. We assume the following relationship between  $\theta$  and  $\beta$  and  $\beta'$

$$\begin{aligned} \sin \beta &= K_1 \sin \theta & \cos \beta &= K_3 \cos \theta \\ \sin \beta' &= K_2 \sin \theta & \cos \beta' &= K_4 \cos \theta \end{aligned}$$

When  $D \ll g\beta H$ , the  $K_i$ 's are products of  $g_{\parallel}$  and  $g_{\perp}$  and  $A$  and  $B$ , the hyperfine constants. We cannot determine  $K_i$  here, as we cannot set any term in  $\mathcal{H}$  equal to zero. Thus we have no additional equations relating  $\theta$ ,  $\beta$ , and  $\beta'$ . The field at resonance is a function of  $\sin \beta$  and  $\cos \beta$ , and since we do not know the relation between  $\beta$  and  $\theta$ , this precludes using  $\mathcal{H}$  to determine  $H_{\text{res}}$  vs.  $\theta$  by a perturbation calculation. We do assume, though, that at  $\theta = 0^\circ$ , all  $K_i$ 's are unity. This allows us to use data at  $\theta = 0^\circ$  to obtain some parameters, although we generally use the standard Hamiltonian for  $D \ll g\beta H$  in this type of calculation.

## Magnetic Resonance Measurements of Proton Exchange in Aqueous Urea<sup>1a</sup>

R. L. Vold,<sup>1b</sup> E. S. Daniel, and S. O. Chan

Contribution from the University of California at San Diego,  
Department of Chemistry, La Jolla, California 92037. Received April 23, 1970

**Abstract:** Rates of protolysis of aqueous urea have been measured by steady-state and spin-echo nmr methods, with good agreement between the two techniques. Below about 2 M urea, the lifetime of a proton on urea is independent of urea concentration. The rate constants for acid-, base-, and water-catalyzed protolysis are  $(9.0 \pm 1) \times 10^6 M^{-1} \text{sec}^{-1}$ ,  $(2.4 \pm 1) \times 10^6 M^{-1} \text{sec}^{-1}$ , and about  $1.5 \pm 0.5 \text{sec}^{-1}$ , respectively. Protonation occurs at urea nitrogen rather than oxygen. Above about 2 or 3 M urea, formation of aggregated species of urea causes the lifetime of a urea proton to depend on urea concentration.

Magnetic resonance measurements have provided detailed information on the rates and mechanisms of proton transfer in aqueous amines<sup>2a</sup> and amides.<sup>2b</sup> Despite its relevance to theories of solution

"structure" and the reversible denaturation of proteins, similar information for urea and substituted ureas is lacking. Most of the nmr rate measurements on amines and amides depend on observation of collapse of spin multiplets of protons coupled to the exchanging protons, and this convenient technique cannot be applied to urea.

In this paper we report measurements of the water and urea nmr line shape. The results are analyzed including explicitly the effect of quadrupole relaxation

(1) (a) We gratefully acknowledge partial support of this work by the Office of Naval Research, under Contract No. N00014-67-A-0200-6021, and the National Science Foundation. (b) Address correspondence to this author.

(2) (a) A. Loewenstein and S. Meiboom, *J. Chem. Phys.*, **27**, 1067 (1957); (b) A. Loewenstein and T. M. Conner, *Ber. Bunsenges. Phys. Chem.*, **67**, 280 (1963).